Organic LETTERS

Letter

pubs.acs.org/OrgLett

Synthesis of a Tetrahydronaphthyridine Spiropyrimidinetrione DNA Gyrase Inhibiting Antibacterial Agent - Differential Substitution at all Five Carbon Atoms of Pyridine.

Gregory S. Basarab,* Vincent Galullo, Nancy DeGrace, Sheila Hauck, Camil Joubran, and Steven S. Wesolowski

Infection Innovative Medicines, AstraZeneca R&D Boston, 35 Gatehouse Drive, Waltham, Massachusetts 02451, United States

Supporting Information

ABSTRACT: The synthesis of (−)-**1**, a potent antibacterial agent, was achieved stereoselectively in nine steps from readily available starting materials. Directed metalations were developed to assemble a pentasubstituted pyridine with appropriately positioned aldehyde and dimethylmorpholine substituents for a key tertiary amino effect reaction (T-reaction) that led to the spirocylic architecture. Ultimately, (−)-**1** was isolated as the thermodynamically most favored stereoisomer.

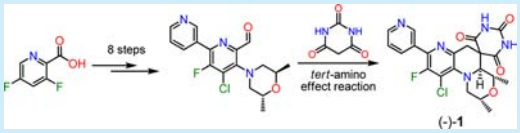

Compound **1** (Figure 1) is a potent antibacterial developed in a medicinal chemistry optimization program[1] to

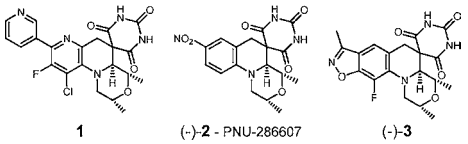

Figure 1. SPT antibacterials **1**, **2**, and **3**.

improve upon the properties of PNU-286607 (**2**), a DNA gyrase inhibitor from Pharmacia-Upjohn showing Gram-positive and fastidious Gram-negative antibacterial activity.[2,3] These and benzisoxazole **3**[4] represent an emerging spiropyrimidinetrione (SPT) class of agents that share the DNA gyrase mode-of-action with fluoroquinolone antibacterials, but differ in their mode of inhibition. Among the bacteria susceptible to the SPT class are *Staphylococcus aureus* (including MRSA, methicillin resistant *S. aureus*), *Streptococcus pneumoniae*, *Streptococcus pyogenes*, and *Haemophilus influenzae*. The spirocyclic architecture of **1**, **2**, and **3** is constructed via the tertiary amino effect reaction (T-reaction) in which a substituent *ortho* to an *N*,*N*-dialkylaniline induces an oxidation of one of the aniline alkyl groups.[5] Reinhoudt first reported a T-reaction wherein Knövenagel adducts of *ortho*-dialkylaniline carboxaldehydes undergo the internal redox reaction ([1,5]-hydride shift) followed by Mannich cyclization to the tetrahydroquinoline ring (Figure 2).[6] The syntheses of **2** and **3** used barbituric acid as the Knövenagel condensation partner

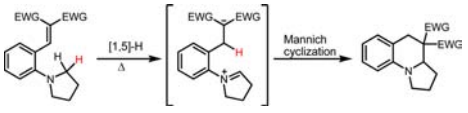

Figure 2. Tertiary amino effect reaction.

with an *ortho*-morpholinyl benzaldehyde.[4,7] Compound **1** with the tetrahydronaphthyridine scaffold, isosteric to the tetrahydroquinoline core of **2**, presented synthetic challenges for the specific substitutions called for by the medicinal chemistry SAR. Toward this end, a series of pyridines were required with a variety of substituents at the 4-, 5-, and 6-positions, an aldehyde at the 2-position, and an amine at the 3-position to set up the T-reaction. Herein we report the assembly of pyridine intermediates with five different substituents through selective pyridine metalation reactions and their conversions to both (±)-**1** and (−)-**1**.

3,5-Difluoropyridine-2-carboxylic acid **4** was envisioned as the starting point toward the synthesis of a 3-amino-2-pyridine aldehyde to set up the final T-reaction. Treating **4** with *cis*-dimethylmorpholine in dioxane at reflux afforded **6** in high yield (Scheme 1). S_NAr displacement of fluoride from the 2-

Scheme 1. Traceless S_NAr Reaction

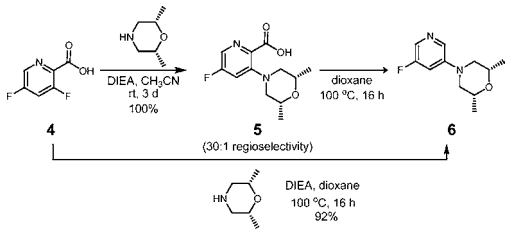

and 4-positions of pyridines occurs straightforwardly due to the inherent electronic activation.[8] However, S_NAr displacement of 3-pyridyl halides is electronically disfavored requiring an activating group *ortho* or *para* to the leaving halide. In the conversion of **4** to **6**, the carboxylate served as a traceless activating group for such displacement. Alternatively, one might

Received: November 13, 2014
Published: December 2, 2014

have considered palladium catalyzed amination of 3-bromo-5-fluoropyridine to **6**,[9] but the traceless activation reaction is simple to run and does not incur the expense and purification issues associated with transition metal catalysis. Displacement of the 3-position fluorine with the morpholine at rt afforded carboxylic acid **5**, which upon heating underwent decarboxylation to afford **6**. Thermal decarboxylation of 2-picolinic acids is known, but proceeds at a considerably higher temperature without the amine substituent.[10] It is noteworthy and useful (see below) that the selectivity of room temperature displacement with morpholine is 30:1 for the 3- over the 5-position fluorine atom due to the carboxylate directing the morpholine nucleophile similar to reported amine displacements of 2,4-difluorobenzoic acids.[11]

Continuing the synthetic sequence from **6** (Scheme 2), a series of directed lithiations were carried out. Though lithiation

Scheme 2. Sequential Lithiations of the Pyridine Ring

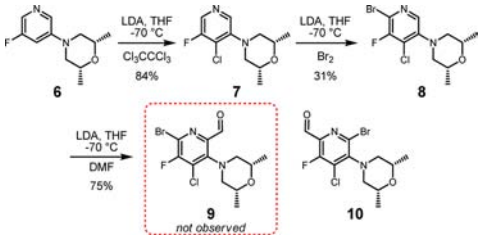

of **6** can occur at the 2-, 4-, or 6-positions, the fluorine atom was presumed to dominate the morpholine as an *ortho*-directing group. Lithiations of 3-fluoropyridine can occur selectively at either the 2- or 4-position depending on reaction conditions with thermodynamic control (LDA in THF) favoring the 4-position.[12] Less certain was whether the morpholine ring of **6** would enhance the lithiation at the pyridine 4-position or, through steric hindrance, drive lithiation to the 2-position. In any event, treatment of **6** with LDA followed by chlorination showed predominant lithiation at the 4-position to give **7**. Subsequent lithiation of **7** occurred selectively next to the fluorine atom as determined by reaction with a brominating reagent to afford **8**, in line with the fluorine operating as a better *ortho*-directing group than the morpholine substituent. Next, treatment of **8** with LDA followed by DMF to install the aldehyde did not lead to the expected **9**, but rather to **10**, the product of bromine migration.[13] Presumably, lithiation proceeded adjacent to the morpholine ring, and bromine migration led to the thermodynamically favored position of lithium next to the fluorine atom.

To circumvent the bromine migration, a modified sequence was developed to **9** for subsequent conversion to (±)-**1** (Scheme 3). Carboxylic acid **5**, the product of room temperature fluorine displacement (Scheme 1), was reduced to the alcohol and protected as the DPS ether **11**. As in Scheme 2, chlorine was introduced onto the pyridine 4-position and bromine onto the 6-position to afford **12**. Deprotection of the alcohol and oxidation led to **9** utilized in a Stille cross-coupling with 3-pyridylstannane to give **13**. Overall the sequences for **6** to **10** and **5** to **9** demonstrated that efficient and selective functionalization of the pyridine ring can be achieved at all five carbon positions. Compounds **9** and **10** are notable in that five different heavy atom types are incorporated at the five positions, perhaps unprecedented. The fluorine, chlorine, and bromine atoms along the synthetic sequences to **9** and **10** offer

Scheme 3. Synthesis of T-Reaction Precursor

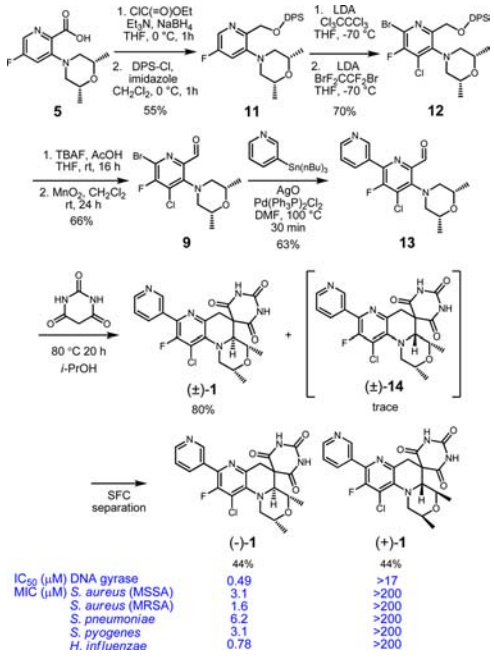

avenues to incorporate other functionality through either S_NAr chemistry or cross-coupling methodology. Clearly, a variety of electrophiles could be envisioned for reaction with lithium intermediates in the sequences, expanding again the range of substituents that can be introduced onto the pyridine ring.

With **13** in hand, the T-reaction was carried out at 80 °C for 20 h leading to (±)-**1** as the predominate product (>95%) with trace **14** (<1%) suggested by ^{19}F NMR. The two optical antipodes of (±)-**1** were separated by chiral SFC purification, and biological activity (inhibition of DNA gyrase and bacterial growth, Scheme 3) resided with (−)-**1** in line with the absolute configurations previously reported for (−)-**2** and (−)-**3**. Notably, the MRSA *S. aureus* strain was also resistant to fluoroquinolone antibacterials including ciprofloxacin (MIC > 50 μM versus MIC = 0.78 for MSSA, methicillin susceptible *S. aureus*). Beyond correlation of activity and rotation with (−)-**2** and (−)-**3**, the absolute configuration of (−)-**1** was also established by an enantiospecific synthesis (see below). Running the T-reaction with **13** for 30 min afforded a 3.4:1 ratio of (±)-**14** and (±)-**1** (see Table 1). Compound **14** was stable as a solid at rt as a mixture with **1**; however, its isolation by chromatography (normal or reversed phase HPLC or SFC) could not be achieved due to facile epimerization to **1**. The configuration of **14** correlated with the minor kinetic material observed during the preparation of (±)-**2**,[7] also not isolated due to configurational instability. Running the T-reaction at 120 °C for 4 h afforded a 28:5.5:1 mixture of (±)-**1**, (±)-**15**, and (±)-**16** as determined by ^{19}F and ^{1}H NMR, the thermodynamic mixture of diastereomers. A trace (~1%) of the fourth possible diastereomer (±)-**14** was suggested by ^{19}F NMR (Table 1).

An enantioselective synthesis of (−)-**1** was achieved starting with the treatment of **4** with chiral (*R,R*)-dimethylmorpholine rather than *meso-cis*-dimethylmorpholine (Scheme 4) and continuing in a sequence analogous to that for (±)-**1**. Reduction of acid **17** and protection of the alcohol to **18** was followed by chlorination and bromination to **19**. Deprotection to the alcohol, oxidation to the aldehyde, and Stille cross-

dx.doi.org/10.1021/ol503256h | Org. Lett. 2014, 16, 6456−6459

Table 1. Distribution of T-Reaction Stereoisomers

13 or 20	Rxtn Temp/ Time	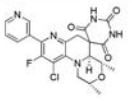 (±)-1	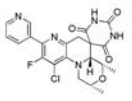 (±)-14	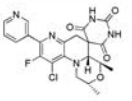 (±)-15	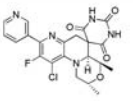 (±)-16
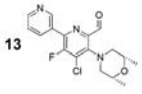 13	80 °C 30 min	23	77	ND[a]	ND
	80 °C 20 h	99%	1%	ND	ND
	120 °C 4 h	79%	1%	16%	3%
		(-)-1	chiral-14	(-)-15	(-)-16
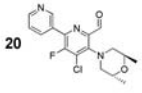 20	80 °C 30 min	ND	ND	42%	58%
	120 °C 4 h	79%	1%	16%	3%

[a]ND = not detected.

Scheme 4. Chiral Synthesis of (−)-1 and Stereoisomers

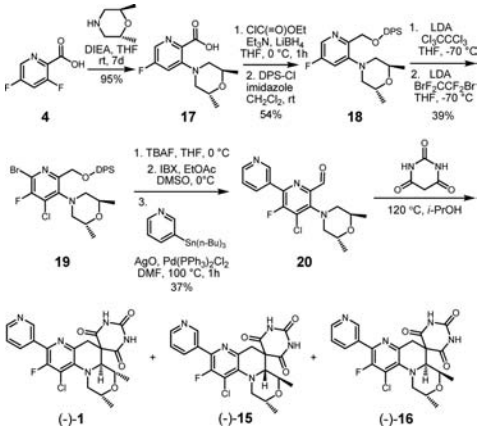

coupling afforded **20**. Heating **20** with barbituric acid at 120 °C for 4 h led to the 28:5.5:1 ratio of (−)-**1** to (−)-**15** to (−)-**16**, the thermodynamic distribution of isomers. Again, a 1% trace of **14** (rotation unknown) could be inferred from the ^{19}F NMR. Running the T-reaction for only 30 min at 80 °C (non-thermodynamic conditions) led to a separable 1.4:1 mixture of (−)-**16** to (−)-**15** (Table 1). Treating purified (−)-**1**, (−)-**15**, or (−)-**16** at 120 °C for 4 h returned the same 28:5.5:1 ratio with perhaps a trace of **14**. This ratio differed from that seen during the preparations of (−)-**2** and (−)-**3** where closer to 9:1 ratios were observed for only the two predominate diastereomers.[4,7] The configurations of (−)-**1**, (±)-**14**, (−)-**15**, and (−)-**16** were determined by detailed NOESY/ROESY analysis. Notably, the conformation for (−)-**15** from the NMR analysis differed significantly from that reported for the analogous minor diastereomer seen under thermodynamic equilibrating conditions during the synthesis of (−)-**3**. The morpholine ring of (−)-**15** adopts a twisted boat conformation with equatorial orientations for the two methyl groups leading to a (1,3)-diaxial NOE for C1 and C4-morpholine H-atoms. The analogous diastereomer of (−)-**3** was shown to exist in a chair conformation with one methyl group being axial and the other being equatorial.[4] The steric influences of chlorine versus fluorine and of the pyridine nitrogen lone pair versus C−H account for the different conformations as well as the difference in diastereomer distribution at thermodynamic equilibrium.

The relative stereochemistry for (−)-**1** using the (*R*,*R*)-dimethylmorpholine of Table 1 was the same as that using the *meso*-dimethylmorpholine for (±)-**1**, which had been rationalized from the mechanism of the T-reaction in the reported synthesis of **2**.[7] Under thermodynamic equilibrating conditions after the Knövenagel condensation and [1,5]-hydride transfer, the methyl group adjacent to the transient iminium species can epimerize as diagrammed in Figure 3. In line with the previous

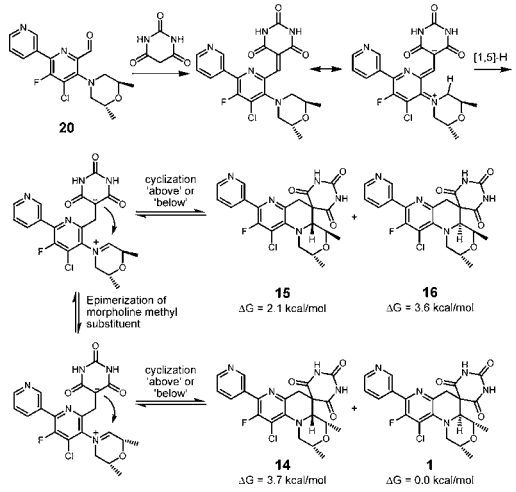

Figure 3. Mechanism of diastereomer equilibration; relative energies of formation.

report for the synthesis of **2**, an equilibrium is established with retro-Mannich opening and closing of the tetrahydronaphthyridine ring. Using a higher 120 °C temperature for the T-reaction versus 80 °C enabled epimerization toward establishing thermodynamic equilibration sampling for all possible diastereomers. The iminium species can collapse by cyclization above and below the morpholine ring with the two methyl groups either *cis* or *trans* to one another. Of the four possible diastereomers, (−)-**1** and (−)-**15** prevail being lowest in energy (see below). The T-reaction with **20** and barbituric acid at 80 °C approached the thermodynamic equilibrium over 4 days indicating that **15** isomerizes more easily than **1**. By contrast, running the T-reaction with *meso*-**13** at 80 °C did not equilibrate to a mixture of (±)-**1** and (±)-**15** even after heating for multiple days, but rather mainly (±)-**1** was isolated.

dx.doi.org/10.1021/ol503256h | *Org. Lett.* 2014, 16, 6456−6459

Nor does heating purified (−)-**1** at 80 °C for longer periods of time lead to isomerization to (−)-**15**. Higher temperatures are necessary to epimerize the methyl of **1** relative to **15**, consistent with the former being more stable than the latter. Shorter, nonthermodynamic 80 °C conditions afforded materials without epimerization of the methyl substituent. Thus, *meso*-**13** led to **1** and **14** maintaining the *cis*-dimethylmorpholine configurations at 80 °C, while chiral **20** formed the two *trans*-dimethylmorpholine diastereomers.

To corroborate the experimental results, the ground state energies of the four possible diastereomers were determined by DFT (def2-TZVPP/M06-2X) calculation, and the relative values in a water solvent model are shown in Figure 3. See Supporting Information (Table S1) for full set of computations in the gas phase and in solvent models using various basis sets and density functionals. The thermodynamically favored diastereomer **1** was used as a reference with the three other diastereomers calculated to have higher energies. Compound **15** was the next most prevalent diastereomer from thermodynamic equilibration corresponding to the next lowest ground state energy from the calculations. The conformations for the four diastereomers calculated by DFT correlated with those determined by NMR analysis (see Supporting Information, S1 p 29−41).

In conclusion, we are aware of only one other report (other than a patent application related to this work)[1] wherein pyridines were utilized in the T-reaction to afford a tetrahydronaphthyridine scaffold.[14] Examples of the T-reaction with other heterocycles have included quinolines, pyrazoles, pyridazines, indoles, and uracils.[15] The sequences developed herein for the syntheses of (±)-**1** and (−)-**1** offer new strategies to fully substitute the pyridine ring. Diastereomer distribution of the T-reaction was shown to depend on substrate stereochemistry and reaction temperature in the context of whether thermodynamic equilibration is reached.

■ ASSOCIATED CONTENT

Supporting Information

Experimental procedures, analytical data, computational methods, and models of the four possible diastereomers. This material is available free of charge via the Internet at http://pubs.acs.org.

■ AUTHOR INFORMATION

Corresponding Author

*E-mail: greg.basarab@astrazeneca.com.

Notes

The authors declare no competing financial interest.

■ ACKNOWLEDGMENTS

The authors are grateful for synthesis of intermediates by Biocon, LTD and GVKBio.

■ REFERENCES

(1) Basarab, G. S.; Dumas, J.; Hill, P. PCT Patent WO 2009004382 A2, 2009.

(2) Miller, A. A.; Bundy, G. L.; Mott, J. E.; Skepner, J. E.; Boyle, T. P.; Harris, D. W.; Hromockyj, A. E.; Marotti, K. R.; Zurenko, G. E.; Munzner, J. B.; Sweeney, M. T.; Bammert, G. F.; Hamel, J. C.; Ford, C. W.; Zhong, W.; Graber, D. R.; Martin, G. E.; Han, F.; Dolak, L. A.; Seest, E. P.; Ruble, J. C.; Kamilar, G. M.; Palmer, J. R.; Banitt, L. S.; Hurd, A. R.; Barbachyn, M. R. *Antimicrob. Agents Chemother.* **2008**, *52*, 2806−2812.

(3) (a) Barbachyn, M. R.; Dobrowolski, P. J.; Hagen, S. E.; Heimbach, T. H.; Hurd, A. R.; Johnson, T. A.; McNamara, D. J.; Ruble, J. C.; Sherry, D. A.; Thomasco, L. M.; Toogood, P. L. PCT Patent WO 2006120563 A2, 2006. (b) Barbachyn, M. R.; Dobrowolski, P. J.; Hurd, A. R.; McNamara, D. J.; Palmer, J. R.; Romero, A. G.; Ruble, J. C.; Sherry, D. A.; Thomasco, L. M.; Toogood, P. L. PCT Patent WO 2004031195 A1, 2004. (c) Johnson, T. A.; Sherry, D. A.; McNamara, D. J.; Toogood, P. L. PCT Patent WO 2007072151, 2007.

(4) Basarab, G. S.; Brassil, P.; Doig, P.; Galullo, V.; Haimes, H. B.; Kern, G.; Kutschke, A.; McNulty, J.; Schuck, V. J. A.; Stone, G.; Gowravaram, M. *J. Med. Chem.* **2014**, *57*, 9078−9095.

(5) Meth-Cohn, O.; Suschitzky, H. In *Heterocycles by Ring Closure of Ortho-Substituted t-Anilines (The t-Amino Effect)*; Advances in Heterocyclic Chemistry; Katritzky, A.R., Boulton, A. J., Eds.; Academic Press: 1972; Vol. *14*, pp 211−278.

(6) (a) Visser, G. W.; Verboom, W.; Benders, P. H.; Reinhoudt, D. N. *J. Chem. Soc., Chem. Commun.* **1982**, 669−671. (b) Verboom, W.; Reinhoudt, D. N.; Visser, R.; Harkema, S. *J. Org. Chem.* **1984**, *49*, 269−276.

(7) Ruble, J. C.; Hurd, A. R.; Johnson, T. A.; Sherry, D. A.; Barbachyn, M. R.; Toogood, P. L.; Bundy, G. L.; Graber, D. R.; Kamilar, G. M. *J. Am. Chem. Soc.* **2009**, *131*, 3991−3997.

(8) (a) Schlosser, M.; Bobbio, C.; Rausis, T. *J. Org. Chem.* **2005**, *70*, 2494−2502. (b) Stroup, B. W.; Szklennik, P. V.; Forster, C. J.; Serrano-Wu, M. *Org. Lett.* **2007**, *9*, 2039−2042.

(9) (a) Navarro, O.; Marion, N.; Mei, J.; Nolan, S. P. *Chem.—Eur. J.* **2006**, *12*, 5142−5148. (b) Samblanet, D. C.; Schmidt, J. A. R. *J. Organomet. Chem.* **2012**, *720*, 7−18. (c) Schrimpf, M. R.; Sippy, K. B.; Daanen, J. F.; Ryther, K. B.; Ji, J. PCT Patent WO 2000071534 A1, 2000.

(10) Dunn, G. E.; Thimm, H. F. *Can. J. Chem.* **1977**, *55*, 1342−1347.

(11) Wendt, M. D.; Kunzer, A. R. *Tetrahedron Lett.* **2010**, *51*, 641−644.

(12) (a) Queguiner, G.; Marsais, F.; Snieckus, V.; Epsztajn, J. In Directed Metalation of Pi-Deficient Azaaromatics: Strategies of Functionalization of Pyridines, Quinolines, and Diazines; *Advances in Heterocyclic Chemistry*; Katrizky, A. R., Ed.; Academic Press: 1991; Vol. *52*, pp 187−304. (b) Mongin, F.; Quéguiner, G. *Tetrahedron* **2001**, *57*, 4059−4090.

(13) (a) Stanetty, P.; Schnuerch, M.; Mereiter, K.; Mihovilovic, M. D. *J. Org. Chem.* **2005**, *70*, 567−574. (b) Schnuerch, M. In *Recent Progress on the Halogen Dance Reaction on Heterocycles*; Iskra, J., Ed.; Topics in Heterocyclic Chemistry, Halogenated Heterocycles; Springer-Verlag: New York, 2012; Vol. *27*, pp 185−218.

(14) Ojea, V.; Muinelo, I.; Figueroa, M. C.; Ruiz, M.; Quintela, J. M. *Synlett* **1995**, *1995*, 622−624.

(15) (a) D'yachenko, E. V.; Glukhareva, T. V.; Dyudya, L. V.; Eltsov, O. V.; Morzherin, Y. Y. *Molecules* **2005**, *10*, 1101−1108. (b) Rabong, C.; Hametner, C.; Mereiter, K.; Kartsev, V. G.; Jordis, U. *Heterocycles* **2008**, *75*, 799−838.